J. Fluid Mech. (1972), *vol.* 55, *part* 4, *pp.* 609–628
Printed in Great Britain

Dissipation and breakdown of a wing-tip vortex

By A. MAGER

The Aerospace Corporation,
El Segundo, California

(Received 11 March 1972)

The solutions of the incompressible quasi-cylindrical momentum-integral equations describing the flow in the viscous core of a wing-tip vortex are obtained in a closed form and are shown to have two distinct branches. The discontinuities of these solutions have infinite axial gradients and therefore, following Hall, are assumed to signal the inception of the vortex breakdown. Benjamin's finite transition, with its excess flow force dissipated, is shown to give results equivalent to a sudden cross-over, upstream of the discontinuity, from one branch solution to another. The critical point of such a cross-over is downstream from the cross-over, at the discontinuity. Sarpkaya's experimental data, and the nature of the solutions ahead of the discontinuity, suggest that the physical manifestation of the discontinuity is the spiral breakdown, whereas the cross-over seems to be related to the rapidly expanding and subsequently contracting axisymmetric bubble. This therefore implies that the beginning of the spiral breakdown is the all important disturbance which triggers off not only the downstream asymmetric departure of the flow from its quasi-cylindrical form but also the formation of the upstream axisymmetric cross-over bubble. Solutions for the turbulent flow downstream from the spiral breakdown indicate that the wing-tip vortex breakdown can result in an appreciable reduction of the maximum circumferential velocity and should thus lessen the danger that trailing vortices present to following aircraft.

1. Introduction

The problem of a vortex with an incompressible viscous core has received considerable attention, as is shown by the reviews of Gartshore (1962), Hall (1966) and Lewellen (1970). Recently, much of this attention has been focused on the so-called vortex breakdown, because it is thought that this phenomenon, though not too well understood, may nevertheless be capable of dissipating the wing trailing vortices. Behind very large aeroplanes these vortices represent a definite but hidden danger to small, following aircraft. A detailed discussion of the various attempts to analyse the vortex breakdown was recently published by Hawkes (1969) and some very beautiful photographs of the various forms of this phenomenon were shown by Sarpkaya (1971). The prevailing picture which appears to be emerging from experimental and analytical approaches is one in which for sufficiently large Reynolds numbers and circulation numbers the

vortex breakdown is viewed as some kind of readjustment between two types of swirling flow: those that do, and those that do not, contain reverse flows. This concept has been proposed, on the basis of his experiments, by Harvey (1962) and analytically rationalized by Benjamin (1962), who by use of elegant mathematics suggested that the inviscid vortex breakdown, like a hydraulic jump, is a transition between two conjugate states of flow.

Vortex breakdown appears to make it impossible to continue the analysis of the viscous core. This has been pointed out by Hall (1967), who showed that the point beyond which the integration of his equations could not be continued was close to an actually observed vortex breakdown. Hall ascribed this failure to the fact that his equations were quasi-cylindrical and therefore could not cope with the very large axial gradients which were occurring just ahead of the breakdown. He further proposed that the failure of the quasi-cylindrical approximation should be interpreted as signalling the onset of the vortex breakdown in a way similar to that in which the failure of the boundary-layer approximation signals the onset of separation. Gartshore (1963), using quasi-cylindrical momentum-integral equations, also encountered singularities beyond which the integration of his equations could not be continued. He, too, suggested that these singularities may be the mathematical indication of the vortex breakdown.

More recently, the quasi-cylindrical momentum-integral equations for the viscous core of the swirling flow through the nozzle were found by Mager (1971*a*) not only to have singularities, but also to yield solutions on both sides of these singularities having the same general characteristics as those of the two conjugate states described by Benjamin. These results then strongly suggested that the integral analysis, by inherently expressing the appropriate conservation laws within the whole core, is well suited to the description of the different states on both sides of the vortex breakdown. Therefore, this analysis may be very expedient for determining the related conditions across the vortex breakdown. To carry this out, the behaviour of the solutions of the quasi-cylindrical momentum-integral equations needed to be investigated more thoroughly and it was for such a purpose that the present work was undertaken.

2. The phase plane

The derivation of the quasi-cylindrical approximation to the complete equations of motion for axially symmetric flow has been given by Hall (1966). This approximation requires that the gradients in the axial direction be much smaller than those in the radial direction, permitting a corresponding neglect of the appropriate terms. Though this process is similar to that which occurs in the boundary-layer approximation, it leads to an important difference, namely, in order to balance the centrifugal force, the static pressure must vary in the radial direction. By indicating dimensional quantities by an overbar and dividing all velocities by the maximum velocity $\bar{Q} = (2\bar{P}_\delta/\bar{\rho})^{\frac{1}{2}}$, all pressures by the maximum dynamic pressure $0{\cdot}5\,\bar{\rho}\bar{Q}^2$ (so that the non-dimensional external total pressure P_δ is unity) and all lengths by the initial core radius $\bar{\delta}_i$, one finds that in terms of cylindrical co-ordinates (r, Θ, z) with corresponding velocity components (u, v, w)

the statements of the conservation of mass and momentum for steady incompressible laminar flow† are

$$(ur)_r + (wr)_z = 0, \quad v^2/r = \tfrac{1}{2}p_r, \tag{1a, b}$$

$$(uvr^2)_r + (vwr^2)_z = \frac{1}{Re}\left[r^2\left(v_r - \frac{v}{r}\right)\right]_r, \tag{1c}$$

$$(uwr)_r + (w^2r)_z = -\tfrac{1}{2}rp_z + (1/Re)\,[r(w)_r]_r, \tag{1d}$$

where $Re = \bar{Q}\bar{\delta}_i/\bar{\nu}$ is the Reynolds number of the laminar flow.

These equations are integrated in the radial direction by assuming that the velocities at the boundary of the core change in a continuous manner into a known potential flow with constant circulation $\Gamma = \bar{\Gamma}/2\pi\bar{\delta}_i\bar{Q}$. This process yields (cf. Mager 1971*a*) the quasi-cylindrical momentum-integral equations for a core of area a, which satisfy the conservation of mass and express the conservation of momentum in the radial, circumferential and axial directions, respectively:

$$p_0 = 1 - (W^2 + V^2 + I_3), \quad I'_{12} = 2/Re, \tag{2a, b}$$

$$I'_{11} + 0{\cdot}5I'_{22} + I_1 W' - (0{\cdot}5\Gamma)^2(a'/a) = 0. \tag{2c}$$

In these equations the prime indicates the total derivative with respect to z, the subscript 0 denotes the values on the axis and the various integrals are defined as

$$I_1 \equiv \int_0^\delta (W - w)\, r\, dr, \quad I_{12} \equiv \int_0^\delta [1 - (vr/\Gamma)]\, wr\, dr,$$

$$I_{11} \equiv \int_0^\delta (W - w)\, wr\, dr, \quad I_{22} \equiv \int_0^\delta v^2 r\, dr, \quad I_3 \equiv 2\int_0^\delta (v^2/r)\, dr.$$

It may be seen from the definition of I_{12} and equation (2*b*) that the angular momentum inside the core is dissipated by the viscous action and that this is due to the assumed constant circulation (Γ) of the external potential flow, which produces an 'effective' torque at the core boundary. This effective torque implies that the circumferential shearing stress does not disappear there and that this stress, for $r > \delta$, must still be supported by the circumferential velocity distribution of the potential flow and be caused by a torque acting on the flow at $r = \infty$. This somewhat unexpected variation of the angular momentum has been thoroughly discussed by Morton (1969), who also pointed out that single unbounded vortices of this type cannot be generated because they would require infinite kinetic energy and would also have infinite angular momentum. Therefore, in nature such vortices do not occur singly but in pairs. For a pair of these vortices, with equal and opposite circulation, the kinetic energy is finite, the angular momentum is zero and the two torques interact at infinity to cancel each other. Of course, for the present investigation it is sufficient to consider only one of the vortices and assume that the other one (except for the direction of rotation) behaves identically. This is the situation which arises in connexion with wing-tip vortices, for which W, the axial velocity outside the core, is

† For turbulent flow the same equations with the real viscosity $\bar{\nu}$ replaced by the eddy viscosity $\bar{\nu}_t$ will be used. This will merely change the Reynolds number to $Re_t = \bar{Q}\bar{\delta}_i/\bar{\nu}_t$.

constant. Thus if we set $\zeta \equiv (2W/Re\,\Gamma^2)\,z$, equations $(2c)$ and $(2b)$ may be integrated to give, respectively,

$$I_{11} + 0{\cdot}5I_{22} - (0{\cdot}5\Gamma)^2 \ln a = \kappa_1, \quad I_{12} - \Gamma^2\zeta/W = \kappa_2, \tag{3}$$

where the integration constant κ_1 may be recognized, after some manipulation, as the invariant flow force deficiency† and κ_2 as the invariant, initial value of the flux of the angular momentum deficiency.

Even though the momentum–integral equations are thus formally integrated, their solution has not really been obtained because the relations between the various integrals ($I_{11}, I_{22}, I_{12}, I_3$) and the core area a are not known. Obviously, additional equations are necessary, and these are provided by specifying the velocities v and w. One may do this by setting

$$w = W[\alpha + (1-\alpha)f_1], \quad v = V(f_2 + \beta f_3), \quad V = \Gamma/\delta,$$

where

$$\eta \equiv r/\delta, \quad f_1 \equiv \eta^2(6 - 8\eta + 3\eta^2), \quad f_2 \equiv \eta(2-\eta^2), \quad f_3 \equiv \eta(1-\eta)^2,$$

and $\delta(\zeta)$ is the radius of the core boundary, $\alpha(\zeta) = w_0/W$ is the form parameter of the axial velocity distribution and $\beta(\zeta)$ is the form parameter of the circumferential velocity distribution. In general, β will be taken as a step function of ζ whose value is a constant and different from zero only behind the vortex breakdown. It should be noted that the above expressions allow the velocities in the core to match the magnitudes as well as the slopes of their corresponding components ($w = W; v = \Gamma/r$) in the external potential flow.

Using these assumptions the integrals become

$$I_{11} = aW^2F_1, \quad I_{12} = aWF_2, \quad I_{22} = \Gamma^2B_1, \quad I_3 = V^2B_2,$$

where the functions F_j and B_j may be written as polynomials in α and β:

$$F_j \equiv K_{j0} + K_{j1}\alpha + K_{j2}\alpha^2, \quad B_j \equiv b_{j0} + b_{j1}\beta + b_{j2}\beta^2,$$

the coefficients K_{ji} and b_{ji} being listed in the appendix.

It is convenient, at this time, to introduce the square of the swirl number $R(\zeta) \equiv (V/W)^2 = \Gamma^2/(aW^2)$ and the functions

$$\theta_1(\zeta) \equiv \kappa_1 + 0{\cdot}25 \ln (\Gamma/W)^2 - 0{\cdot}5B_1, \quad \theta_2(\zeta) \equiv \kappa_2 + \zeta.$$

Of these, θ_2 is easily identifiable as the local flux of the angular momentum deficiency. To see the physical meaning of θ_1, consider the fact that in the present formulation, owing to the assumed stepwise variation of β, θ_1 is also a step function, changing only behind the vortex breakdown. Thus ahead (or in the absence) of vortex breakdown, θ_1 may be used as a measure of the invariant flow force deficiency. Substituting into (3) and $(2a)$ we thus obtain

$$F_1 = R(\theta_1 - 0{\cdot}25 \ln R), \quad F_2 = R\theta_2, \tag{4a, b}$$

$$p_0 = 1 - W^2[1 + R(1 + B_2)]. \tag{4c}$$

† This name is used following Benjamin, who called $\bar{S} \equiv 2\pi \int_0^{\bar{\delta}} (\bar{p} + \bar{\rho}\bar{w}^2)\,\bar{r}\,d\bar{r}$ the flow force. It should be noted, however, that since the static pressure at the core boundary varies κ_1 and $\bar{S}$ are not obviously interchangeable.

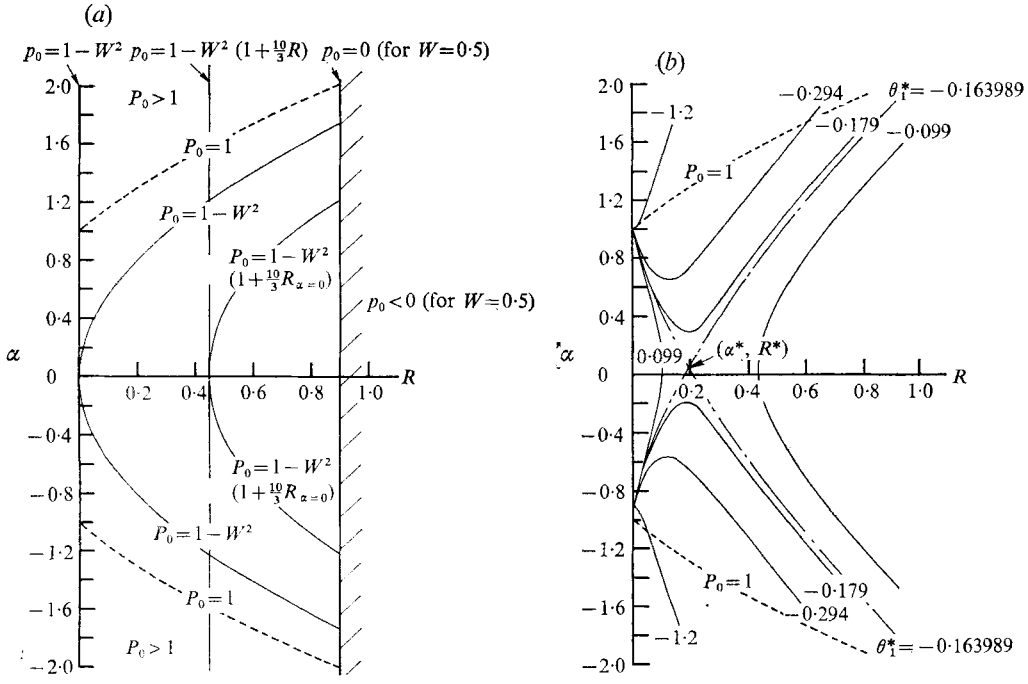

FIGURE 1. Lines of (a) constant total and static pressure on the axis and (b) constant flow force deficiency κ_1 (e.g. θ_1) in the phase plane. Solid curves in (b) are labelled with values of θ_1.

We can see from (4c) that the lines of constant p_0 coincide with the lines of constant R and also, since the total pressure P_0 on the axis is given by

$$P_0 = p_0 + (\alpha W)^2 = 1 - W^2[1 - \alpha^2 + R(1+B_2)],$$

that the lines of constant P_0 are given by parabolas symmetric about the R axis and translated for larger values of P_0 towards smaller values of R. These are shown in figure 1 (a).

Considering now the α, R plane, usually known as the phase plane,† and realizing that the flow cannot exist for $p_0 < 0$ (because all pressures are absolute), we see that the region in which the solutions can exist is bounded by $R = 0$ (flow without swirl) and by the maximum value $R_m = (1-W^2)/[W^2(1+B_2)]$ ($p_0 = 0$). In addition, when the flow inside the core has the same total pressure as that outside ($P_\delta = 1$),‡ then this region is also limited by the parabolas connecting the points $\alpha = \pm 1$, $R = 0$ and $\alpha = \pm[1+R_m(1+B_2)]^{\frac{1}{2}}$, R_m, which are the lines on which $P_0 = 1$. All these limits are shown in figure 1 (a).

† The reason for this designation will become clear when the connexion with the differential equations is discussed.

‡ This may or may not be the case when jet engines are located close to the wing tip.

3. Solution of the axial momentum equation

Turning our attention to (4*a*), we note that since K_{12} is not zero it too represents some form of the quadratic in the α, R plane. In particular, by defining a transcendental function $\tau \equiv R(\theta_1 - 0{\cdot}25 \ln R)$ we obtain distorted parabolas

$$\alpha = \alpha^* \pm [(\tau - \tau^*)/K_{12}]^{\frac{1}{2}}, \tag{5}$$

where $\alpha^* = -0{\cdot}5K_{11}/K_{12}$, $\tau^* = K_{10} - 0{\cdot}25K_{12}(K_{11}/K_{12})^2$.

Since K_{12} is negative, τ must always be smaller than τ^*. However, the function τ has a maximum at $R = \exp(4\theta_1 - 1)$ so there must be a special value of the flow force deficiency κ_1^* (and thus also θ_1^*) beyond which regions of R in which the solution cannot exist will appear. For $\theta_1 = \theta_1^*$, the two (hereafter called upper and lower) separate branches of (5) meet at $\alpha_u = \alpha_l = \alpha^*$ and $R = R^* = 4\tau^*$, so that for all $\theta_1 > \theta_1^*$ the upper and lower branches remain joined.

One should note from the relations in the appendix that, regardless of the particular form of the axial velocity profile (e.g. choice of f_1), $K_{12} = -(K_{11} + K_{10})$. Because of this interdependence, for $R = 0$ (e.g. either infinitely large a, or $\Gamma = 0$) all upper- and lower-branch solutions pass through

$$\alpha_u = 1 \quad \text{and} \quad \alpha_l = -(1 - 2\alpha^*),$$

respectively. Thus, when the swirling flow is completely dissipated all upper-branch solutions result in uniform axial flow $w = W$, while all lower-branch solutions give strongly reversed flow on the axis. The slight asymmetry, with respect to $\alpha = 0$, which also produces $P_{0,l} < P_{0,u}$, is dependent on the particular choice of f_1 and therefore may, or may not, be real.

Figure 1 (*b*) illustrates the behaviour of (5) and shows that, when the flow force deficiency is too large, the core of the quasi-cylindrical flow cannot satisfy the conservation of the axial momentum for certain intermediate values of R, and that the region in which this occurs lies on both sides of R^*. One should also observe that, because $\alpha^* > 0$, reversed flow on the axis (e.g. $\alpha < 0$) cannot occur for upper-branch solutions with $\theta_1 < \theta_1^*$.

4. Continuous solutions of the system

We note that since $K_{22} = 0$, the solution of (4*b*) is given by a straight line

$$\alpha = (R\theta_2 - K_{20})/K_{21}, \tag{6}$$

which rotates, as ζ increases from its initial value ζ_i, in the counter-clockwise direction about the point $\alpha = -K_{20}/K_{21}$, $R = 0$. This rotation is the analytical representation of the viscous dissipation which produces the ever larger value of θ_2, that is, the ever growing axial flux of the angular momentum deficiency. For inviscid flow $Re = \infty$ and θ_2 remains equal to its initial value κ_2, so that the line given by (6) does not rotate.

Clearly, then, the solution of the system (4*a*, *b*) is given by the intersection of (5) and (6), thus indicating that the flow always requires a certain definite

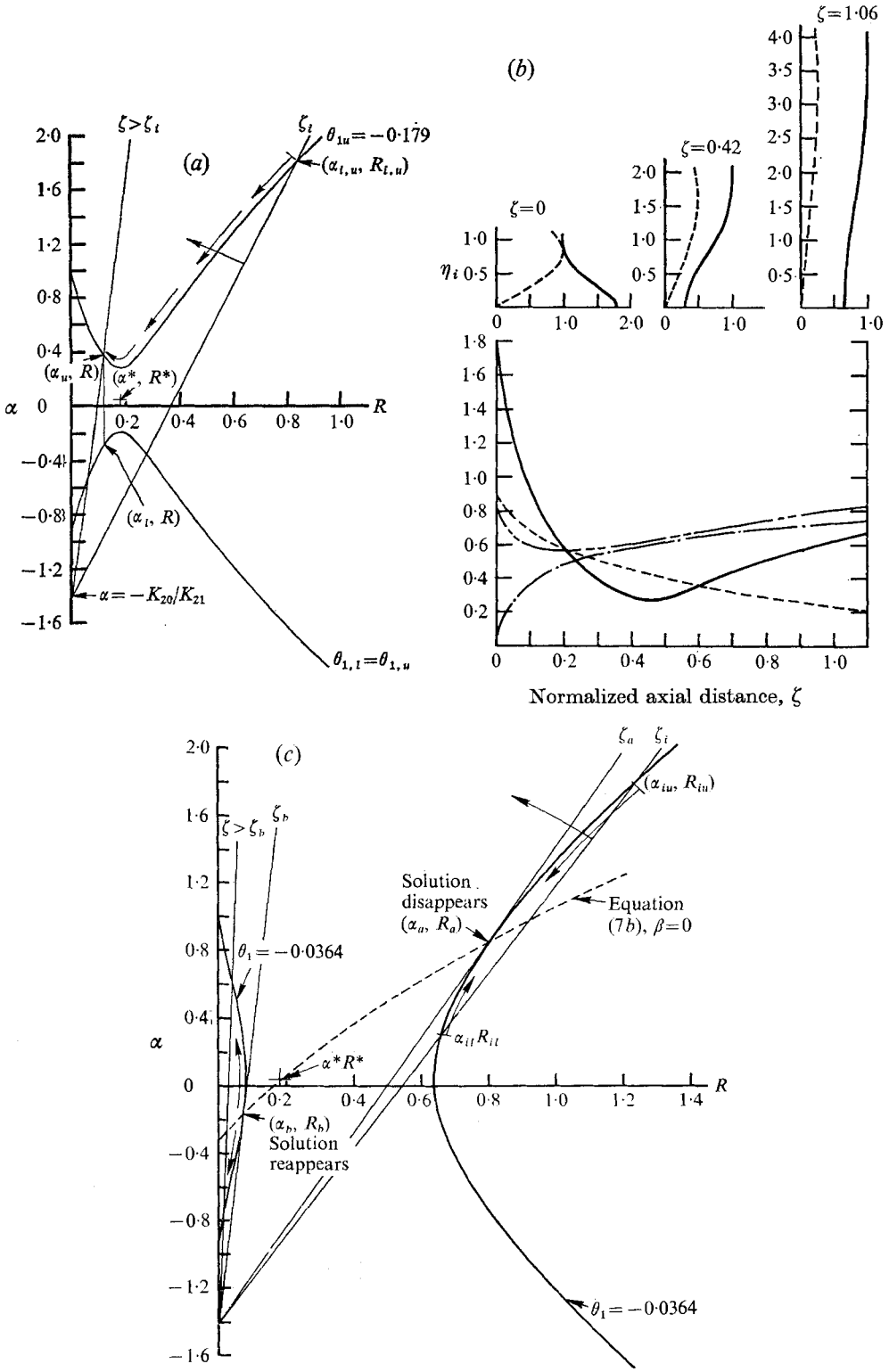

FIGURE 2. (*a*) Continuous solutions of the system ($\theta_1 < \theta_1^*$) in the phase plane. (*b*) Continuous solution in the physical plane for $\zeta_i = 0$, $\alpha_i = 1{\cdot}80$, $R_i = 0{\cdot}84$ (e.g., $\theta_1 = -0{\cdot}179$). In upper diagrams: ——, w/W; – – –, v/W. In lower diagram: ——, w_0/W; – – –, V/W; —·—, p_0; — — — —, P_0. (*c*) Discontinuous solutions of the system ($\theta_1 > \theta_1^*$) in the phase plane.

balance between its angular momentum and its flow force. This process is shown in figure 2(*a*).

Assume that the initial values α_i, R_i at ζ_i are such that when substituted into (4*a*) they yield $\theta_1 \leqslant \theta_1^*$. This means that the initial point will lie on one of the separate branches of (5) and that the solution can proceed uninterrupted along this branch towards lower and lower values of R as the line (6) rotates towards $R = 0$. Thus one obtains for each ζ the corresponding $\alpha(\zeta)$ and $R(\zeta)$ from which all velocities and pressures may be determined. In practice, of course, it is unnecessary to rely on this geometrical construction. For each set of initial conditions one determines θ_1 and κ_2. Next, (5) yields $\alpha(R, \theta_1)$ and this, in turn, when substituted into (6) gives $\theta_2(\alpha, R)$ and therefore $\zeta(\alpha, R)$.

The velocities and pressures found thus for the upper branch of figure 2(*a*) are shown as a function of the axial distance in figure 2(*b*). It may be seen in figures 2(*a*) and (*b*) that these continuous solutions describe the dissipation of the swirling motion with steadily increasing static pressure on the axis. This viscous decay of the vortex wake is consistent with the results obtained by other investigators (cf. Hall 1965; Bossel 1970).

As R decreases toward R^*, the absolute value of the axial velocity on the axis tends to decrease and then, as R decreases further, it increases again. This decrease of $|w_0|$ is most pronounced when $\theta_1 \approx \theta_1^*$, e.g. when the flow force deficiency is large. Under these conditions the total pressure, and hence the total energy, initially tends to decrease and then remains nearly constant (see figures 2(*b*) and 1(*a*)). Apparently, when the flow force deficiency is large, the energy which the swirling wake is able to gain by expansion into the outer potential flow is not sufficient to satisfy its own internal requirements. As a result of the decreasing (or even constant) total pressure and the simultaneously increasing static pressure, both the axial and the circumferential velocities decrease. The existence of this coupling has been previously pointed out by Morton (1969).

For $R < R^*$ the total pressure increases in the downstream direction so that, for the upper-branch solutions, at the downstream infinity $P_{0,u} = 1$ (but $P_{0,l} < 1$) and the energy recovers its free-stream value at all radii.† Thus for small circumferential velocities, the vortex wake, by expanding into the outer potential flow, gains more energy than is necessary to satisfy its own internal requirements. However, the static pressure is essentially uniform throughout the core and tends very slowly towards $1 - W^2$. $|w_0|$ must thus increase in parallel with the increasing total pressure, and the coupling between the axial and circumferential velocities disappears.

At the downstream infinity, where the swirling motion is completely dissipated, the flow in a core of a wing-tip vortex must have an axial velocity which is everywhere equal and opposite to the velocity of the aeroplane. Since this condition is satisfied only on the upper branches we see that the lower branches of the continuous solutions do not yield physically realistic representation of the flow in the core of a wing-tip vortex. One should, however, note that when

† Such recovery also occurs when a non-rotating wake is dissipated by the viscous action [see, for example, Goldstein (1950)].

$\theta_1 = \theta_1^*$ the passage from the lower to the upper branch at $\alpha = \alpha^*$ and $R = R^*$ is possible, so that under these special conditions the lower-branch solution can yield physically significant results.

5. Flow ahead of vortex breakdown

As was discussed previously, when the initial conditions are such that the flow force deficiency is too large (e.g., $\theta_1 > \theta_1^*$), the upper and lower branches are joined and there appears a region where the real solutions of (4*a*) cannot exist. Let us now assume that $R_i > R^*$ so that as ζ increases the two solutions on the joined branches of the θ_1 curve more towards each other until they meet at (α_a, R_a), when the line ζ_a is just tangent to the curve θ_1. This is shown in figure 2(*c*). Since ζ can only increase, it is obvious that the solution cannot be continued beyond this point and that it ceases to exist until at some other $\zeta = \zeta_b$ (say) the line ζ_b again becomes tangent to the second part of the θ_1 curve at point (α_b, R_b). From this point on, the solutions are continuous and spread apart on the two branches of the θ_1 curve for all $\zeta > \zeta_b$. Thus, when $\theta_1 > \theta_1^*$ and $R_i > R^*$, the solutions of the system, regardless of the branch on which they start, are discontinuous, terminating at (α_a, R_a) and starting again at (α_b, R_b).

It is important to note that, in general, $\alpha_a > 0$, so that the discontinuity occurs when the flow is not actually stagnated on the axis. A failure of the equations when the flow is still not stagnated has also been obtained by Hall (1967) and Bossel (1970).† This misbehaviour of the analysis is thus different from that experienced in the computations of the boundary layer, where an actual stagnation point at the surface signals the onset of separation. In spite of this fact, Hall ascribed this failure to the inability of the quasi-cylindrical approximation to cope with the very large axial gradients which he obtained there and suggested that it indicates the beginning of the vortex breakdown. Because of this argument it is important to know the precise values of α and R at which such discontinuities occur. This may be done by equating the values of $d\alpha/dR$ given by (5) and (6). After some manipulation one obtains

$$4K_{21}F_3 + R = 0, \tag{7a}$$

whose solution is

$$\alpha = -K_{20}/K_{21} \pm 0{\cdot}5[(R^{**} - R)/K_{12}]^{\frac{1}{2}}, \tag{7b}$$

where $R^{**} \equiv 4[K_{10} - K_{11}K_{20}/K_{21} + K_{12}(K_{20}/K_{21})^2]$. We thus see that the values of α and R at the discontinuity are affected only by the constants K_{ji} (and hence by the assumed velocity distributions f_1, f_2 and f_3), but are completely independent of the Reynolds number or the values of the invariants κ_1 and κ_2. Also, as is illustrated in figure 2(*c*), the plot of (7*b*) (for $\beta = 0$ and using plus sign only) passes through (α^*, R^*), so that the flow solutions terminate (we shall use subscript a to denote termination) whenever $\alpha = \alpha_a > \alpha^*$ and $R = R_a > R^*$.

In order to clarify the causes of this failure of the quasi-cylindrical analysis it is appropriate to check whether the basic assumptions of such an analysis remain valid at, or near, the discontinuities. This is conveniently done by

† In spite of the fact that Hall did not use momentum–integral method and Bossel employed a series of exponentials in his calculations.

inserting the expressions for the integrals I_{ij} into the differential equations (2*c*) and (2*b*). After differentiation this results in the system

$$(2K_{12}\alpha + K_{11})\,\alpha' + (0{\cdot}25 - F_1/R)\,R' = 0, \tag{8a}$$

$$K_{21}\alpha' - (F_2/R)\,R' = R, \tag{8b}$$

which shows that α' and R' will be infinite whenever the determinant of their coefficients is zero. Such vanishing of this determinant occurs when (7*b*) is satisfied, thus showing that the quasi-cylindrical analysis fails because the flow attains very large axial gradients. Since such large axial gradients must clearly be present somewhere within the region of the vortex breakdown depicted in the photographs of Harvey (1962), Sarpkaya (1971) and others, we shall assume, in line with Hall's (1967) idea, that the failure of the quasi-cylindrical analysis is an indication of the occurrence of the vortex breakdown. Thus for the flow to undergo the vortex breakdown its R_i must be larger than the value of R at which the line of its α_i intersects the curve θ_1^* [e.g. $R_i \geqslant R(\theta_1^*, \alpha_i)$]. This is shown in figure 3(*a*), where for any given set of initial conditions (α_i, R_i) the path to the conditions at discontinuity (α_a, R_a) is also indicated.

It is pertinent to note here that Bossel (1968) proposed a criterion which separates those vortex flows which will decay smoothly from those which will undergo vortex breakdown. According to his analysis, vortex breakdown will eventually occur whenever $[(dv/dr)_0\delta/w_0]_i = 2(R_i/\alpha_i)^{\frac{1}{2}}$ is larger than a certain value. For uniform flow ($\alpha_i = 1$), this reduces to the requirement that R_i be larger than $\frac{1}{2}$, while figure 3(*a*) shows that $\alpha_i = 1$ intersects θ_1^* at $R_i = 0{\cdot}51$, which agrees very well with Bossel's result.

In a later paper, Bossel (1971) showed that for uniform flow the value of $(dv/dr)_0\delta/w_0$ at which his equations became singular (e.g. all derivatives became infinite in magnitude and reversed their sign) and at which the vortex breakdown was thought to occur was 1·8. This compares directly to the value of 1·915 which represents the first singularity of the inviscid equations describing the core of a swirling flow through the nozzle rotating like a solid body. The occurrence of this singularity was suggested by King (1967) to be caused by the vortex breakdown and had also been previously found by Fraenkel (1956). Using Bossel's values at $\alpha_a = 1$ one obtains $R_a = \frac{1}{4}(1{\cdot}8)^2 = 0{\cdot}81$. On the other hand, figure 3(*a*) shows that, at $\alpha_a = 1$, $R_a = 0{\cdot}95$, which compares somewhat better with King's criterion $\frac{1}{4}(1{\cdot}92)^2 = 0{\cdot}92$ than with Bossel's value.

By considering the nature of the flow just ahead of the discontinuity one gains additional insight into the physical conditions preceding the formation of this phenomenon. These conditions are shown in figure 3(*b*), where typical flow on upper and lower branches, for the same axial flux of the angular momentum deficiency θ_2 and circulation Γ, is illustrated. As may be seen in this figure, on the upper branch, a strong adverse static pressure gradient produces a rapid deceleration of the axial flow and an expansion of the core. On the lower branch, however, the static pressure, though much higher, is almost constant except very near the discontinuity, where it tends to decrease. Because of this and because of the very slightly increasing total pressure, the axial flow accelerates

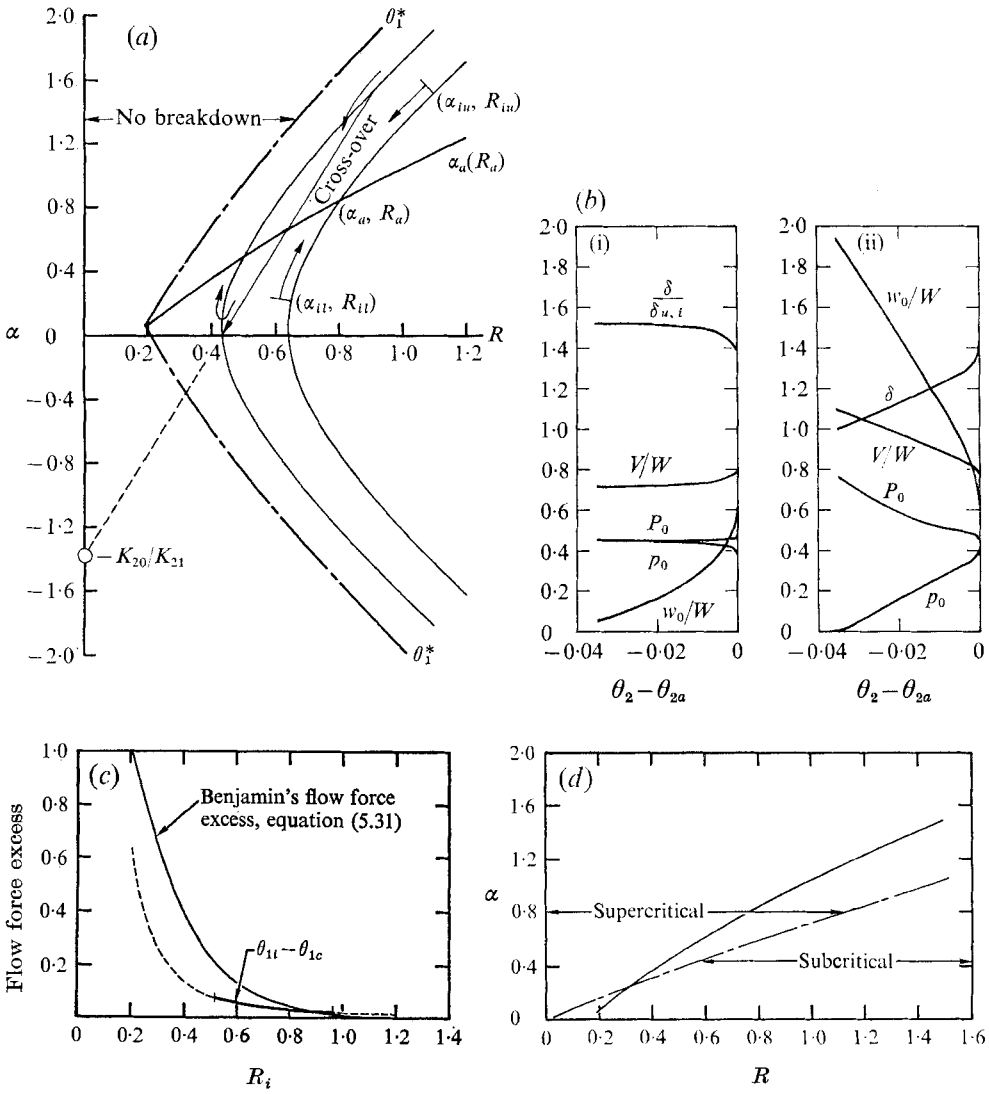

FIGURE 3. (*a*) Effect of initial conditions on the occurrence of vortex breakdown. (*b*) Flow upstream of discontinuity; $\alpha_a = 0{\cdot}628$, $R_a = 0{\cdot}611$, $W = 0{\cdot}45$, $\Gamma_u = \Gamma_l$. $\theta_2 - \theta_{2a}$ axial flux of the angular momentum deficiency. (i) Lower branch. (ii) Upper branch. (*c*) Comparison of flow force excess. (The extension of $\theta_{1i} - \theta_{1c}$ to continuous solutions is indicated by the broken line.) (*d*) Comparison of $\alpha_a(R_a)$ (solid line) with Benjamin's critical line (broken line).

and the core, which is much larger than on the upper branch, shows a tendency to collapse. This inclination of the core to expand on the upper branch and to contract slightly on the lower branch, together with the presence of characteristic axisymmetric 'bubbles' (which are formed by a rapid expansion of the flow followed by immediate contraction) in the many photographs of vortex breakdown, suggest that, just ahead of the discontinuity, at a fixed ζ and thus at the same θ_2, the flow may be crossing over from the upper- to the lower-branch solution (see figure 3(*a*)). Of course, one cannot expect such a sudden

cross-over to be properly described by the present quasi-cylindrical analysis. However, once it occurs, the flow conditions behind it should be those of the lower-branch solution, which must still lead to the discontinuity. Hypothesizing, therefore, that the bubble represents such a cross-over, one should expect downstream of the bubble an acceleration of the axial flow, followed by a second strong disturbance which should be there even when the bubble does not exist. Indeed, in the photographs of Sarpkaya (1971, figures 9–11) one observes that a strong disturbance downstream of the bubble is always present, even before the bubble is 'born', and that the dye filament between it and the bubble has a tendency to disappear, as it would if the flow were accelerating. Thus the photographic evidence appears to confirm our hypothesis and furthermore suggests that the analytical discontinuity may be related to the disturbance always visible behind the bubble and usually referred to as the 'spiral breakdown'. Moreover, this same photographic evidence appears to indicate that the cross-over from the upper to the lower branch is in fact caused (e.g. the bubble is formed when the downstream disturbance is already present) by the disturbance at the discontinuity. Since such a triggering effect is very reminiscent of a hydraulic jump and also since Sarpkaya has actually stated that the bubble is Benjamin's finite transition, it is appropriate to investigate whether our cross-over is equivalent to such a finite transition.

To this end Benjamin's (1962, example 2, for a tube of infinite radius, pp. 620–622) results for the present case may be stated (using our nomenclature) as follows. For an initially supercritical flow with $\alpha_i = 1$ transitions will occur for all $R_i \leqslant 1{\cdot}44$. These transitions will terminate in a conjugate subcritical flow having a flow force excess† and are given by

$$\alpha_c = 1-(1{\cdot}44-R_i)/1{\cdot}2J_1(2{\cdot}4), \quad R_c = (R_i/1{\cdot}2)^2.$$

Should Benjamin's transitions, after the dissipation of the excess flow force, be equivalent to our cross-over, they must (i) lie on a family of straight lines all intersecting in a common origin located close to our origin $\alpha = -K_{20}/K_{21}$, $R = 0$ and (ii) have an excess flow force which behaves like $\theta_{1i}-\theta_{1c}$. (An exact agreement between the two is not expected because θ_1 is not the flow force.) Furthermore, our upper- and lower-branch solutions would have to correspond to Benjamin's supercritical and subcritical regimes, respectively. One should now note that α_c is a linear function of R_i whose origin is at $\alpha_c \approx -1{\cdot}3$, $R_i = 0$, which compares well with our value of $-K_{20}/K_{21} \approx 1{\cdot}38$, so that the first condition is clearly satisfied. To check the second condition, we plot in figure 3(*c*) Benjamin's (1962, equation (5.31), p. 622) expression for the flow force excess together with the difference $\theta_{1i}-\theta_{1c}$, as computed from (α_i, R_i) and (α_c, R_c). As may be seen in this figure, though Benjamin's solution is inviscid and linearized, the two tend to vary in a very similar manner. Consequently, we may interpret figure 3(*c*), together with the previous test, as an indication that the intersection of our lower-branch solutions with the line of fixed ζ would give results which would behave like those of Benjamin, once his excess of flow force were dissipated.

† Benjamin indicates that in reality this excess will be dissipated by wave formation or by the total pressure loss and this dissipation is not included in his analysis.

Finally, to show that the upper-branch solutions are supercritical, we use Benjamin's test function ϕ. The flow is subcritical when this function, in addition to its initial value $\phi(0) = 0$, has at least one zero in the interval $0 \leqslant \eta \leqslant 1$. Transforming to the present formulation, Benjamin's equation for ϕ becomes

$$\Phi'' - \Phi'/\eta + (8W\Phi/w)\,[3\eta(1-\eta)\,(1-\alpha) + RW(2-3\eta^2+\eta^4)/w] = 0,$$

which, when solved with $\Phi(0) = \Phi'(0) = 0$ for various values of α and R, permits the determination of the boundary between supercritical and subcritical flow regimes. This boundary is compared in figure 3 (*d*) with the locus of the terminating discontinuity $\alpha_a(R_a)$ which separates our branch solutions. Again, though the two do not match too well, particularly for large R, it is clear from figure 3 (*d*) that our upper- and lower-branch solutions have the same relationship to $\alpha_a(R_a)$ as the supercritical and subcritical regimes have to Benjamin's critical line.

We may thus conclude from the above comparisons that the cross-over from the upper to the lower branch of the discontinuous solutions gives results which are equivalent to the finite transition proposed by Benjamin, once the excess flow force of such a transition is dissipated. Furthermore, it is pertinent to point out here that, if the upper-branch solutions are supercritical and the lower-branch solutions subcritical, then it follows that the critical point for each cross-over (e.g. one with the same flow force deficiency as the primary flow) is located at the discontinuity and thus is downstream from the cross-over. This helps to explain why the spiral breakdown appears to be causing the formation of the bubble, as is indicated by Sarpkaya's photographs.

As a result of the above discussion it is clear that the point at which the quasi-cylindrical equations fail and which, according to Hall, signals the start of vortex breakdown is the point at which the asymmetric spiral breakdown (and not the axisymmetric bubble) begins. The spiral breakdown, however, appears to be the all important disturbance which is responsible not only for the downstream departure from the quasi-cylindrical flow, but also, when the conditions are right, for the upstream formation of the transition bubble. It occurs because the quasi-cylindrical flow is unable to match its available flow force with its ever increasing angular momentum deficiency. Thus the occurrence of the spiral breakdown is the result of the viscous dissipation, though the cross-over which it sometimes causes is essentially an inviscid phenomenon.

6. Flow behind vortex breakdown

The photographs of Sarpkaya and others clearly show that the spiral breakdown rapidly loses its asymmetric features through violent turbulent mixing. One may thus expect that a short distance downstream the flow is again axisymmetric. This is confirmed by the data of Hummel (1965), who made his measurements behind the vortex breakdown of a delta wing. Such axisymmetric, though turbulent, flow should again be describable by our quasi-cylindrical analysis and therefore the proper conditions at the starting point (henceforth designated by subscript *d*) for such a downstream solution are needed. These

should be obtainable by observing that the conservation laws must remain valid across the breakdown and therefore should yield a set of relations properly connecting the conditions ahead of the breakdown (α_a, R_a) with those at the start of our solution (α_d, R_d).

To obtain these relations we shall first assume that the expressions given previously for the laminar velocity profiles are still applicable to the mean velocities of the turbulent flow, but that the actual viscosity $\bar{\nu}$ is replaced by the eddy viscosity $\bar{\nu}_t$. According to Hall (1966), the ratio $\epsilon = \bar{\nu}_t/\bar{\nu}$ has been shown by Owen to remain roughly constant when $\bar{\Gamma}/\bar{\nu}$ is invariant. Consequently, the equations derived above remain unchanged, except that now $\zeta_t = \epsilon\zeta$. Since ϵ is generally one to three orders of magnitude larger than unity, we see that the turbulent flow increases the rate at which the angular momentum is dissipated with z. However, we shall assume here that the downstream flow returns to quasi-cylindrical form in a negligible distance, so that this increased rate can have no effect on the initial value of the local flux of the angular momentum deficiency θ_2, and we must put $\kappa_{2d} = \kappa_{2a} - (\zeta_d - \zeta_a) = \kappa_{2a} - \zeta_a(\epsilon - 1)$ to ensure this.† Furthermore, since the statement of the conservation of the axial momentum does not involve ζ the flow force deficiency κ_1 remains unchanged.

We thus have $\theta_{2d} = \theta_{2a}$ and $\kappa_{1d} = \kappa_{1a}$. To satisfy these requirements the present analysis proposes that the spiral breakdown and the resulting change to turbulent flow suddenly distort not only the axial, but also the circumferential velocity profiles. This distortion is analytically introduced by a step increase of β, from zero before the breakdown, to a new constant value which, as yet, is undetermined. It is important to note that, since the coefficients of F_1 are independent of B_j, the only effect that such a change will have on the solution of the axial momentum equation is to produce a step decrease of θ_1. Thus, though the flow force deficiency κ_1 will remain invariant, the axial momentum equation behind the breakdown will behave as if the flow had a lower flow force deficiency than that ahead of the breakdown. Similarly, since the coefficients of F_2 are B_3 and B_4 but θ_2 is invariant, the angular momentum equation behind the vortex breakdown will, with increasing β, shift its origin along the $R = 0$ axis towards $\alpha > -1{\cdot}38$. It is thus obvious that by suitable adjustment of β one may always find a point on any of the other θ_1 lines which satisfies $\theta_{2d} = \theta_{2a}$ and $\kappa_{1d} = \kappa_{1a}$. As an example, the loci of such points for $\alpha_a = 0{\cdot}480$, $R_a = 0{\cdot}491$ are shown in figure 4 and it is clear that additional constraints are required to choose the correct starting conditions for the downstream solution from the many possible ones.

To make this choice we assume first that at downstream infinity the flow must be uniform (e.g., $\alpha = 1$ at $R = 0$) and second, that the vortex breakdown produces a strong deceleration of the flow on the axis (e.g. $\alpha_d \ll 1$). These

† To obtain a solution across the vortex breakdown the author (1971*b*) has previously proposed joining the terminating and starting discontinuities having the same value of κ_1. Such a connexion requires $\theta_{2d} > \theta_{2a}$. However, a sudden change in θ_2 is inadmissible (this was first pointed out to the author by Prof. G. Carrier) because it implies a sudden change in the tangential stress distribution (and thus the circumferential velocity distribution) of the potential flow and therefore is inconsistent with the original assumptions of the analysis.

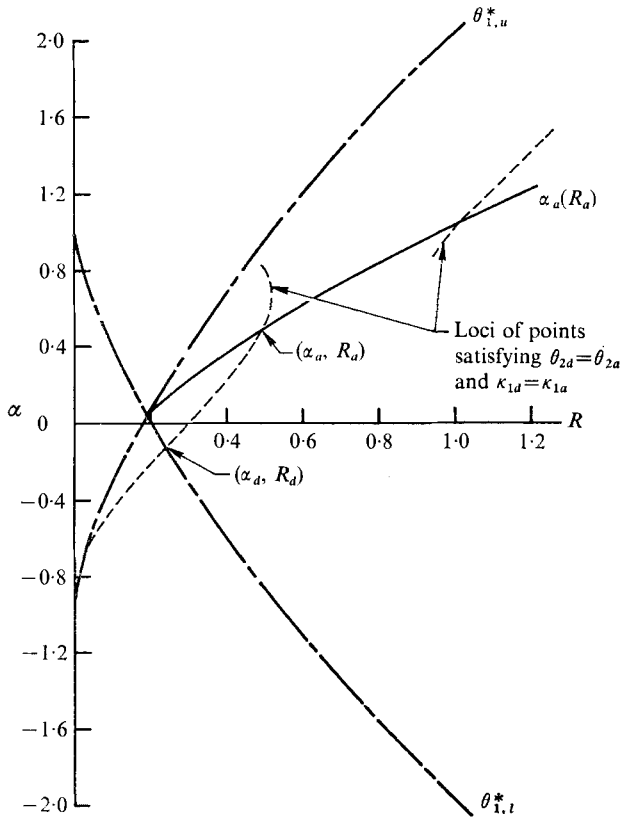

FIGURE 4. Loci of points satisfying the invariance of angular momentum and flow force deficiency.

assumptions are justified by the fact that at infinity, where the vortex wake is completely dissipated, the velocity must be that of the aeroplane, and also by the many photographs of the spiral breakdown, all showing a definite stagnation point on the axis. These two requirements are sufficient to determine our starting conditions for the downstream solution and the only point which can satisfy them is obviously the one lying on $\theta^*_{1,l}$ (see figure 4). Setting, therefore, $\theta_{1d} = \theta^*_1$ and solving for β, one obtains

$$\beta = -b_{11}/2b_{12} + [(b_{11}/2b_{12})^2 + 2(\theta_{1a} - \theta^*_1)/b_{12}]^{\frac{1}{2}}, \tag{9}$$

and this value, when substituted into (4*b*) and (5), together with $\theta_{2d} = \theta_{2a}$, determines α_d and R_d.

It should be obvious that once its starting conditions are determined, the downstream solution may be continued along the θ^*_1 line in the described manner except, as previously mentioned, that ζ_t and κ_{2d} must now be used instead of ζ and κ_2, respectively. It is also pertinent to point out here that, though the locus of the discontinuities $\alpha_a(R_a)$ will be affected by the value of β, this approximates a counterclockwise rotation of the $\alpha_a(R_a)$ line about (α^*, R^*), so that it will not produce any discontinuities in our downstream solution.

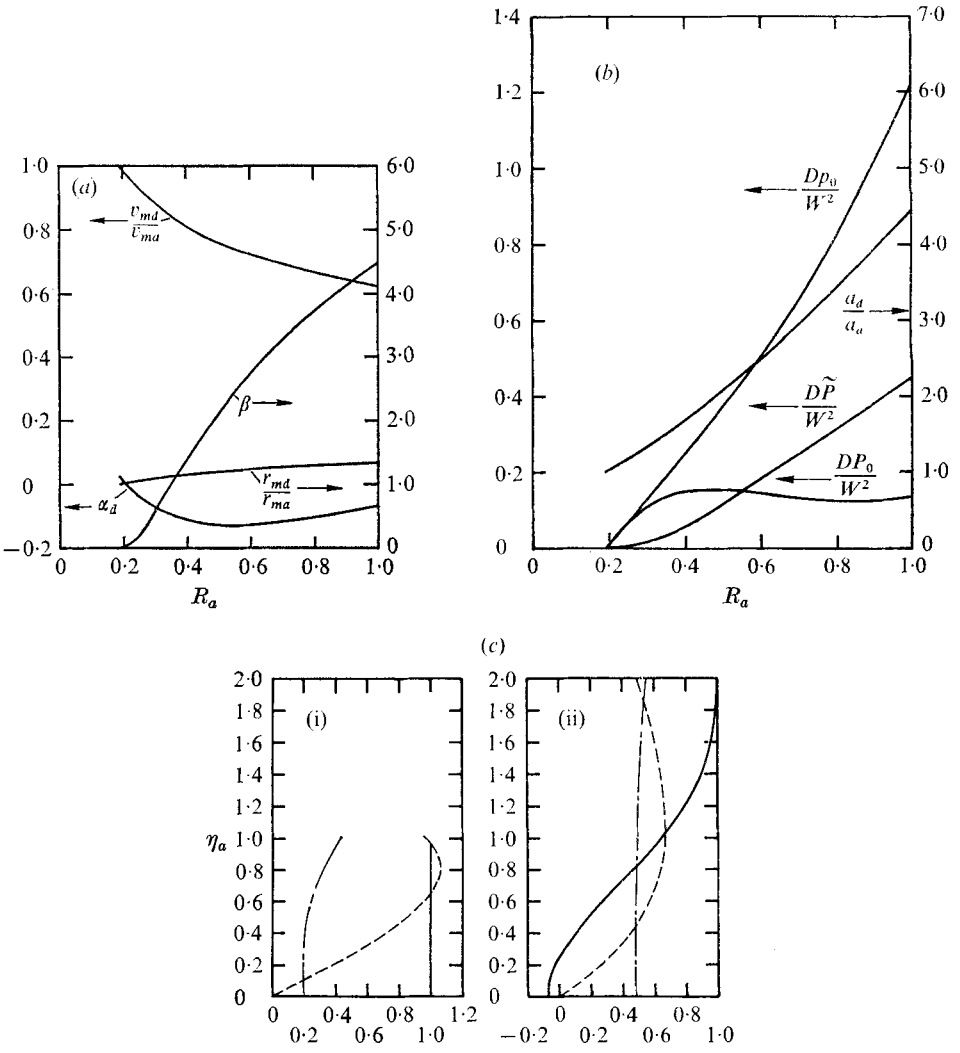

FIGURE 5. Effect of breakdown on (*a*) core velocities and (*b*) core area and pressure rise. (*c*) Changes of velocity and pressure distributions across vortex breakdown, $\alpha_a = 1$, $R_a = 0{\cdot}95$, $W = 0{\cdot}45$. ——, w/W; – – –, v/W ;—·—, $p/(1-W^2)$. (i) Ahead of breakdown. (ii) Downstream from breakdown.

The results of such computations for α_d and R_d are shown in figure 5(*a*), which summarizes the effect of breakdown on the core velocities. In particular, since α_d is negative it is obvious that, near the axis, the downstream solution starts with a slightly reversed flow. This effect, however, tends to diminish for large R_a, that is, when the breakdown becomes strong. Figure 5(*a*) also shows that, in spite of the strongly increasing β, the maximum circumferential velocity v_m decreases and the radius r_m at which this velocity is located varies but little. This reduction of the circumferential velocity implies that the occurrence of vortex breakdown will help to lessen the danger which the wing-tip vortices represent to following aircraft.

Similarly, figure 5(*b*) shows that the vortex breakdown results in a substantial expansion of the core, an appreciable static pressure rise on the axis

$$Dp_0 \equiv p_{0d} - p_{0a}$$

and a somewhat smaller increase of the average total pressure in the core.† This figure also indicates a rather small increase of the total pressure on the axis. Apparently, the core gains energy by suddenly expanding and turbulently mixing with the potential flow.

Finally, figure 5(*c*) shows the changes in the velocity and pressure distributions for the case when the axial flow ahead of the breakdown is uniform ($\alpha_a = 1$). As may be seen from this figure, vortex breakdown produces extensive distortions of both the axial and the circumferential velocity distributions and a virtual equalization of the static pressure in the core.

7. Summary of findings

(i) Closed-form transcendental solutions of the quasi-cylindrical momentum-integral equations for the flow in the viscous core of a wing-tip vortex are shown to have two separate branches with the same flow force deficiency. However, at the downstream infinity, where the swirling motion is completely dissipated, only one (the upper) of these branches yields solutions with a uniform axial velocity equal and opposite to the velocity of the aeroplane. The other branch gives solutions with a strongly reversed flow on the axis. When the flow force deficiency has a certain special value, a smooth passage from one branch to the other is possible.

(ii) When the value of the flow force deficiency is larger than the special value, the two separate branches join and at their junction discontinuities appear in the solutions. These discontinuities have infinitely large axial gradients with which the quasi-cylindrical equations cannot cope and therefore are identical to the breakdown-signalling singularities found by Hall (1967) and others.

(iii) Benjamin's (1962) finite transition, with its excess flow force dissipated, is shown to give results which are equivalent to a cross-over, upstream of the discontinuity and at a fixed ζ, from the upper- to the lower-branch solution. Furthermore, the critical point for such a cross-over, which has the same flow force deficiency as the primary flow, is located at the discontinuity and therefore downstream from the cross-over. This means that the upper-branch solutions are supercritical and the lower-branch solutions subcritical, and implies that the disturbance at the discontinuity is responsible for the occurrence of the cross-over.

(iv) Upstream of the discontinuity, the upper-branch solution results in a strongly decelerating flow with a rapidly expanding core while the lower-branch solution (with same angular momentum) gives accelerating flow with a substantially larger but slightly contracting core. These facts, together with Sarpkaya's (1971) photographs and observations that the axisymmetric bubble is always

† The average total pressure in the core is independent of the circumferential velocity distribution and is given by $\tilde{P} \equiv 2\int_0^1 P\eta\, d\eta = 1 - W^2(1+R-F_4)$.

followed by the spiral breakdown, suggest that the spiral breakdown may be the physical manifestation of the discontinuity, while the axisymmetric bubble may be related to the cross-over. The inception of the asymmetric spiral breakdown is thus seen to be the all important disturbance responsible for the formation of the upstream bubble and also producing its own, downstream departure from the quasi-cylindrical flow. The equations show that this occurs because of the flow's inability to match its ever increasing (owing to the viscous effect) flux of angular momentum deficiency with its available flow force.

(v) Downstream from the spiral breakdown, where the flow has returned to axial symmetry through a turbulent mixing process, the starting-point for a new continuous turbulent flow solution is obtainable from the conditions ahead of the discontinuity by (*a*) ensuring the preservation of the flow force and angular momentum deficiencies, (*b*) requiring the downstream solution to yield uniform axial flow at infinity, and (*c*) requiring that the axial velocities near the axis be low.

(vi) The results thus obtained show that the wing-tip vortex breakdown causes a pronounced distortion of the axial and circumferential velocity profiles, expansion of the core, large static pressure rise on the axis and some recovery of the total pressure. Furthermore, the breakdown causes a substantial reduction of the maximum circumferential velocity and therefore it should be beneficial in lessening the danger that wing-tip vortices represent to following aircraft.

Appendix. Constants and coefficients

Define

$$k_i \equiv \int_0^1 f_1^l f_2^m f_3^n \eta^t \, d\eta,$$

then the integration yields the values of k_i given in table 1.

i	l	m	n	t	k_i
1	1	0	0	1	$\frac{4}{10}$
2	2	0	0	1	$\frac{111}{315}$
3	0	1	0	2	$\frac{1}{3}$
4	1	1	0	2	$\frac{191}{630}$
5	0	2	0	1	$\frac{11}{24}$
6	0	2	0	−1	$\frac{7}{6}$
7	0	1	1	1	$\frac{23}{840}$
8	0	0	2	1	$\frac{1}{280}$
9	0	0	1	2	$\frac{1}{60}$
10	1	0	1	2	$\frac{31}{2520}$
11	0	1	1	−1	$\frac{3}{20}$
12	0	0	2	−1	$\frac{1}{12}$

TABLE 1. The constants k_i

Using these values of k_i we can obtain the values of the coefficients b_{ji} and K_{ji} given in tables 2 and 3.

j	$i\ldots$	0	1	2
1		k_5	$2k_7$	k_8
2		$2k_6$	$4k_{11}$	$2k_{12}$
3		k_1-k_4	$-k_{10}$	0
4		$0{\cdot}5-k_1-k_3+k_4$	$k_{10}-k_9$	0

TABLE 2. The coefficients b_{ji}

j	$i\ldots$	0	1	2
1		k_1-k_2	$0{\cdot}5-3k_1+2k_2$	$2k_1-k_2-0{\cdot}5$
2		B_3	B_4	0
3		$K_{20}K_{11}/K_{21}K_{12}-K_{10}/K_{12}$	$2K_{20}/K_{21}$	1
4		$2k_2$	$4(k_1-k_2)$	$1-4k_1+2k_2$

TABLE 3. The coefficients K_{ji}

Other important quantities are evaluated as:

$$\alpha^* = 0{\cdot}045454, \quad R^* = 0{\cdot}190909, \quad \theta_1^* = -0{\cdot}163989,$$

$$\tau^* = 0{\cdot}047727, \quad R^{**} = -0{\cdot}238636.$$

REFERENCES

BENJAMIN, T. B. 1962 Theory of the vortex breakdown phenomenon. *J. Fluid Mech.* **14**, 593–629.

BOSSEL, H. H. 1968 Stagnation criterion for vortex flows. *A.I.A.A. J.* **6**, 1192–1193.

BOSSEL, H. H. 1970 Use of exponentials in the integral solution of the parabolic equations of boundary-layer, wake, jet and vortex flows. *J. Comp. Phys.* **5**, 359–382.

BOSSEL, H. H. 1971 Vortex computation by the method of weighted residuals using exponentials. *A.I.A.A. J.* **9**, 2027–2034.

FRAENKEL, L. E. 1956 On the flow of rotating fluid past bodies in a pipe. *Proc. Roy. Soc.* A**233**, 506–526.

GARTSHORE, I. S. 1962 Recent work in swirling incompressible flow. *Nat. Res. Lab. Can. Rep.* LR–343.

GARTSHORE, I. S. 1963 Some numerical solutions for the viscous core of an irrotational vortex. *Nat. Res. Counc. Can., Aero. Rep.* LR–378.

GOLDSTEIN, S. (ed.) 1950 *Modern Developments in Fluid Dynamics.* vol. II, pp. 571–574. Oxford University Press.

HALL, M. G. 1965 A numerical method for solving the equations for a vortex core. *Min. Tech. Lond. R. & M.* no. 3467.

HALL, M. G. 1966 The structure of concentrated vortex cores. *Progress in Aeronautical Science* (ed. D. Kucheman), vol. 7, pp. 53–110. Pergamon.

HALL, M. G. 1967 A new approach to vortex breakdown. *Proc.* 1967 *Heat Transfer and Fluid Mechanics Institute*, pp. 319–340. Stanford University Press.

HARVEY, J. K. 1962 Some observations of the vortex breakdown phenomenon. *J. Fluid Mech.* **14**, 585–592.

HAWKES, J. W. 1969 A simple model for the vortex breakdown phenomenon. M.S. thesis, Dept. Aero. and Astro., MIT.

HUMMEL, D. 1965 Untersuchungen über das Aufplatzen der Wirbel an schlanken Deltaflügeln. *Z. Flugwiss.* **13**, 158–168.

KING, W. S. 1967 A theoretical investigation of swirling flows through a nozzle. Ph.D. dissertation, University of California, Los Angeles.

LEWELLEN, W. S. 1970 A review of confined vortex flows. *MIT Space Propulsion Lab. Rep.* no. 70–1.

MAGER, A. 1971*a* Incompressible, viscous, swirling flow through a nozzle. *A.I.A.A. J.* **9**, 649–655.

MAGER, A. 1971*b* Solution across vortex breakdown. *Aerospace Rep.* ATR–71(9999)–1.

MORTON, B. R. 1969 The strength of vortex and swirling core flows. *J. Fluid Mech.* **38**, 315–333.

SARPKAYA, T. 1971 On stationary and travelling vortex breakdown. *J. Fluid Mech.* **45**, 545–559.